

# Heat and Mass Transfer due to Natural Convection along a Wavy Vertical Plate with Opposing Thermal and Solutal Buoyancy Effects

M. Si Abdallah<sup>1</sup> and B. Zeghmati<sup>2</sup>

**Abstract:** In the present work, a numerical analysis is performed of the combined effects of (opposing) thermal and solutal buoyancy in the presence of a wavy (vertical) surface. The boundary layer equations and related boundary conditions are discretized using a finite volume scheme and solved numerically using a Gauss-Seidel algorithm. The influence of the wavy geometry (in terms of related wavelength  $L$  and amplitude  $a$ ) and the buoyancy ratio  $N$  on the local Nusselt and Sherwood numbers and on the skin-friction coefficient are studied in detail. Results show that when  $Pr < Sc$ , negative values of the buoyancy parameter,  $N$  tend to increase the local Nusselt number and the skin-friction coefficient. An increase in the parameter  $a$  leads to a reduction in the heat and mass transfer and the local skin-friction coefficient. For  $N < 0$  and  $Pr > Sc$ , the flow is completely perturbed; the thickness of the mass boundary layer is larger than that of the thermal boundary layer.

**Keywords:** free convection, boundary layer, buoyancy force, vertical wavy surface.

## 1 Introduction

Natural convection along a surface due to combined temperature and solutal variations has received considerable attention in recent years because of its importance in a wide range of scientific fields such as biology, oceanography, astrophysics, geology, chemical processes and crystal-growth techniques, as reported by [Marcoux et al. (1998); Mamou (2003); Markus (2004)].

Previous studies of natural convection and related heat and mass transfer mechanisms have focused mainly on a flat plate or on uniform channels.

---

<sup>1</sup> Corresponding author: Physics Department, Faculty of Sciences, University of M'Sila, Algeria .  
Email: s\_maayouf@yahoo.fr

<sup>2</sup> Laboratoire de Mathématiques et Physique, Université de Perpignan Via Domitia, France.

[Adams et al. (1966)] experimentally studied free convection with opposing body forces. [Bottemanne (1971)] developed some steady-state theoretical solutions for  $Pr=0.71$  and  $Sc=0.63$ . [Gebhart and Pera (1971)] elaborated a general formulation of the vertical two-dimensional boundary layer flows.

[Callahan and Marner (1976)] studied the free convection with mass transfer on a vertical flat plate with  $Pr=1$  and a realistic range of Schmidt numbers. [Chen and Yuh (1980)] presented locally nonsimilar solutions for natural convection along a vertical cylinder. [Mahajan and Angivasa (1993)] studied the natural convection along a heated surface with opposing buoyancies.

These results demonstrated that boundary-layer solutions cannot yield accurate solutions for natural convection flows with opposing buoyancies. Moreover, the heat and mass transfer rates follow complex trends depending on the buoyancy ratio.

[Ching-Yang Cheng (2000)] analysed the free thermal and mass transfer near a vertical wavy surface with a constant wall temperature and concentration in a porous medium. These results showed that an increase in the buoyancy ratio tends to increase both the Nusselt and Sherwood numbers.

[Jer-Huan J. et al (2003)] analysed this problem in the case of a vertical wavy surface. The wavy surface was maintained at uniform wall temperature and constant wall concentration. A marching finite-difference scheme was used for the analysis. It was found that higher amplitude–wavelength ratios increase the fluctuation of velocity, temperature and concentration fields. However, the local skin-friction, Nusselt number and Sherwood number are smaller for the larger amplitude–wavelength ratios.

[Kefeng and Wen-Qiang (2006)] numerically analyzed the influence of the buoyancy ratio  $N$  on the double-diffusive convection in a vertical cylinder with radial temperature and axial solute gradients for different values of  $Gr$ ,  $Pr$  and  $Sc$ . [Hossain et al (1998)], analyzed the heat transfer response of free convection flow from a vertical heated plate to an oscillating surface heat flux. [SiAbdallah et al (2011)] studied natural convection in the boundary layer along a vertical cylinder with opposing buoyancies. Results showed that the Nusselt (Sherwood) number increases with positive or negative buoyancies ratio. [Al-Ajmi and Mosaad (2012)] analyzed heat transfer across a vertical solid wall separating natural convection in a cold fluid-saturated porous medium and film condensation in a saturated-vapour medium. They found that increasing the wall thermal parameter reduces the heat transfer performance of both heat transfer modes. The Lattice Boltzmann method was applied on natural convection in an inclined triangular cavity for different thermal boundary conditions by [Mahmoudi et al (2013)]. A numerical study of mixed convection in an open partitioned heated cavity was performed by [Mahrouche et

al (2013)]. Results showed that the flow and heat transfer depend significantly on Reynolds number and the block height. [Dihmani et al (2012)] numerically investigated natural convection with surface radiation in a vented vertical channel heated asymmetrically. The numerical solution was obtained using a finite volume method based on the SIMPLER algorithm. The increase of the rib width was found to decrease the average hot wall Nusselt number, while the radiation exchange increases the dimensionless temperature. Other interesting studies are due to [Hamimid, Guellal, Amroune and Zeraibi, (2012); Moufekkir, Moussaoui, Mezrhab, Naji and Bouzidi, (2012); Choukairy and Bennacer, (2012); Arid, Kouksou, Jegadheeswaran, Jamil, Zeraoui, (2012); Shemirani and Saghir (2013); Maougal and Bessaïh, (2013); Kamath, Balaji and Venkateshan (2013); Rtibi, Hasnaoui and Amahmid, (2013); Rana and Thakur (2013); Haslavsky, Miroshnichenko, Kit, and Gelfgat (2013)].

## 2 Model description

Consider a semi-infinite vertical wavy plat as shown schematically in Fig.1. The wavy surface of the plate is described by  $y=f(x) = a.\sin(2\pi x)$ , where  $a$  is the amplitude of the wavy surface and  $L$  is the characteristic wavelength. The surface is maintained at a uniform temperature  $T_w$  and concentration  $c_w$  which are different than the ambient values,  $T_\infty$  and  $c_\infty$ . The buoyancy forces induced by the gradients of temperature and concentration give rise to the flow. The origin of the Cartesian coordinates system  $(x, y)$  is placed at the leading edge of the surface. The values  $u$  and  $v$  are the velocity components in the  $x$  and  $y$  direction respectively. The fluid is assumed to have constant physical proprieties except for the density variation in the buoyancy term of the momentum equation.

## 3 Mathematical governing equations

The governing equations for a steady, laminar and incompressible flow along a vertical wavy surface with the Boussinesq approximation may be written as:

Continuity equation

$$\frac{\partial u}{\partial x} + \frac{\partial v}{\partial y} = 0 \quad (1)$$

Momentum equation

$$u \frac{\partial u}{\partial x} + v \frac{\partial u}{\partial y} = -\frac{1}{\rho} \frac{\partial p}{\partial x} + \nu \left( \frac{\partial^2 u}{\partial x^2} + \frac{\partial^2 u}{\partial y^2} \right) + g\beta_t(T - T_\infty) + g\beta_c(c - c_\infty) \quad (2)$$

$$u \frac{\partial v}{\partial x} + v \frac{\partial v}{\partial y} = -\frac{1}{\rho} \frac{\partial p}{\partial y} + \nu \left( \frac{\partial^2 v}{\partial x^2} + \frac{\partial^2 v}{\partial y^2} \right) \quad (3)$$

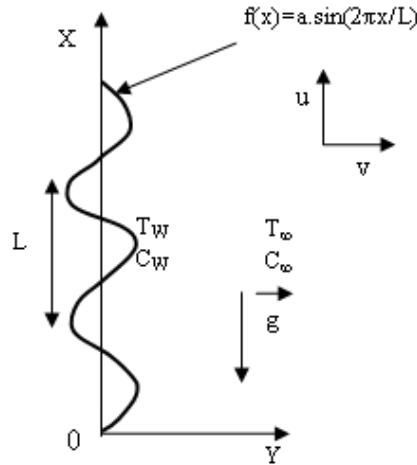


Figure 1: Physical model and coordinate system.

Energy Equation

$$u \frac{\partial T}{\partial x} + v \frac{\partial T}{\partial y} = \alpha \left( \frac{\partial^2 T}{\partial x^2} + \frac{\partial^2 T}{\partial y^2} \right) \quad (4)$$

Concentration equation

$$u \frac{\partial c}{\partial x} + v \frac{\partial c}{\partial y} = D \left( \frac{\partial^2 c}{\partial x^2} + \frac{\partial^2 c}{\partial y^2} \right) \quad (5)$$

The appropriate boundary conditions for the problem are:

$$y=f(x): u=0, v=0, T= T_w, c=c_w$$

$$y \rightarrow \infty: u=0, T= T_\infty, c=c_\infty$$

We now introduce the following dimensionless variables:

$$X = \frac{x}{L}; \quad Y = \frac{y}{L} Gr^{1/4}; \quad A = \frac{a}{L}, \quad F(X) = A \sin(2\pi X)$$

$$U = \frac{L}{\nu Gr^{1/2}} u; \quad V = \frac{L}{\nu Gr^{1/4}} v; \quad P = \frac{\rho L^2}{\mu^2 Gr} p, \quad (6)$$

$$Gr = \frac{g \beta_t (T_w - T_\infty) L^3}{\nu^2}$$

For the current problem, Eq. (3) indicates that the pressure gradient along the y direction is of  $O(Gr^{-1/4})$ , which indicates that the lowest order pressure gradient

along x direction can be determined from the inviscid flow solution, however, since there is no externally imposed free stream, this pressure gradient is zero. Therefore, the term  $(\partial p/\partial y)$  may be eliminated from Eqs. (3) and (4), resulting the following system of equations:

$$U \frac{\partial U}{\partial X} + V \frac{\partial V}{\partial Y} = 0 \quad (7)$$

$$U \frac{\partial U}{\partial X} + V \frac{\partial U}{\partial Y} = \frac{\partial^2 U}{\partial Y^2} + \theta + NC \quad (8)$$

$$U \frac{\partial \theta}{\partial X} + V \frac{\partial \theta}{\partial Y} = \frac{1}{Pr} \frac{\partial^2 \theta}{\partial Y^2} \quad (9)$$

$$U \frac{\partial C}{\partial X} + V \frac{\partial C}{\partial Y} = \frac{1}{Sc} \frac{\partial^2 C}{\partial Y^2} \quad (10)$$

Equation (8) shows that when N is equal to zero, there is no mass diffusion body force and the problem reduces to pure heat convection; when N becomes infinite, there is no thermal diffusion; when  $N < 0$ , the mass diffusion buoyancy forces oppose those of thermal diffusion and when  $N > 0$ , the mass diffusion buoyancy forces aid those of thermal diffusion.

In order to remove the singularity at the leading edge [Yao L.S. (1983)], the following transformations are used

$$\xi = X; \quad \eta = \frac{Y - F(X)}{(4X)^{1/4}} \quad (11)$$

In the new coordinate system  $(O, \xi, \eta)$  the equations (7-10) become:

$$U \frac{\partial U}{\partial \xi} + \eta_x \frac{\partial U}{\partial \eta} + \eta_y \frac{\partial V}{\partial \eta} = 0 \quad (12)$$

$$U \frac{\partial U}{\partial \xi} + (\eta_x U + V \eta_y) \frac{\partial U}{\partial \eta} = (\eta_y)^2 \frac{\partial^2 U}{\partial \eta^2} + \theta + N.C \quad (13)$$

$$U \frac{\partial C}{\partial \xi} + (\eta_x U + V \eta_y) \frac{\partial C}{\partial \eta} = \frac{\eta_y^2}{Sc} \frac{\partial^2 C}{\partial \eta^2} \quad (14)$$

where

$$\eta_x = \frac{\partial \eta}{\partial X} = \frac{-F' - \eta \cdot (4X)^{-3/4}}{(4X)^{1/4}}, \quad F_x = \frac{\partial F}{\partial X} \quad (15)$$

$$\eta_y = \frac{\partial \eta}{\partial Y} = \frac{1}{(4X)^{1/4}}$$

The corresponding boundary conditions are:

$$\eta = 0; \quad U = V = 0; \quad \theta = 1; \quad C = 1 \eta \rightarrow \infty : U = 0; \quad \theta = 0, \quad C = 0 \quad (16)$$

After obtaining the velocity, temperature and concentration fields along the wavy surface. The Nusselt number, Sherwood number and the local skin-friction coefficient are the important parameters in this problem. These parameters are defined in the new coordinate  $(0, \xi, \eta)$  system as:

$$Nu = -\frac{Lq_w}{k(T_w - T_\infty)}$$

where  $k$  is thermal conductivity and  $q_w$  is the heat flux at the wall given by:

$$q_w = k \vec{n} \cdot \nabla T$$

here

$$\vec{n} = \left\{ -\frac{F_x}{\sqrt{1 + F_x^2}}, \frac{1}{\sqrt{1 + F_x^2}} \right\} \quad (17)$$

where  $\mathbf{n}$  is the unit vector normal to the wavy surface. Using boundary layer variables (6) and (16), we obtain

$$Nu_x = -(1 + F_x^2)^{1/2} \left( \frac{Gr}{4X} \right)^{1/4} \left( \frac{\partial \theta}{\partial \eta} \right)_{\eta=0} \quad (18)$$

and the local Sherwood number can be written as follow:

$$Sh_x = -(1 + F_x^2)^{1/2} \left( \frac{Gr}{4X} \right)^{1/4} \left( \frac{\partial C}{\partial \eta} \right)_{\eta=0} \quad (19)$$

the local skin-friction coefficient is defined by:

$$Cf_x = 2 \frac{\tau_w}{\rho \tilde{U}^2} \quad (20)$$

$$\tau_w = \left[ \mu \left( \frac{\partial u}{\partial y} + \frac{\partial v}{\partial x} \right) \right]_{y=0} \quad (21)$$

Substituting Eq. (22) into Eq. (21) in terms of dimensionless quantities, we obtain

$$Cf_x = 2 \left( \frac{4X}{Gr} \right)^{1/4} \left( \frac{\partial U}{\partial \eta} \right)_{\eta=0} \quad (22)$$

#### 4 Numerical method

In this work, a marching finite volume scheme was used to discretize the coupled equations (12-15) for  $U$ ,  $\theta$  and  $C$ . Moreover, grid independency checks were made. Some of the calculations were tested using  $200 \times 250$  nodes in the  $X$  and  $Y$  directions respectively but no significant improvement over the use of  $120 \times 150$  grid points was found. The algebraic system of equations are solved using Gauss-Seidel algorithm with a relaxation coefficient equal to 0.7 for the variable  $U$  and to 0.5 for  $\theta$  and  $C$ . During the program test, the convergence criterion used was  $|\Phi^{k+1} - \Phi^k| / \sum \Phi^{k+1} \leq 10^{-5}$ , where  $\Phi^k$  and  $\Phi^{k+1}$  are the values of the  $k^{th}$  and  $(k+1)^{th}$  iterations of  $U$ ,  $\theta$  and  $C$ . Furthermore, the numerical scheme used in this work is checked.

Our computational results for aiding and opposing buoyancies for the mean Nusselt and Sherwood numbers were compared with the experimental data ( $Pr=0.7$ ,  $Sc=2.23$ ) for opposing flow which were obtained for a vertical smooth surface ( $A=0$ ) by [Adams and Mc.Fadden (1966)] as well as with the numerical results obtained by [Mahajan and Angirasa (1993)] as reported in Table 1.

Table 1: Comparison of Nu and Sh numbers for a vertical surface for  $N=-0.43$ .

	Nu	Sh
Present work	25.24	41.30
[Adams and Mc.Fadden (1966)]	24.38	42.10
[Mahajan and Angirasa (1993)]	23.03	41.44

#### 5 Results and discussion

The controlling parameters of the fluid flow and heat and mass transfer rates for this problem are the Prandtl number  $Pr$ , Schmidt number  $Sc$ , buoyancy ratio ( $N = Gr_c/Gr_t$ ) and the amplitude wavelength  $A$  for the wavy surface as described by  $f(x) = A \sin(2\pi X)$ . The numerical results for the velocity, temperature and concentration fields are presented. Hence, the inadequacies of the boundary layer analysis are specified. Moreover, we present comprehensive results of the local friction coefficient, local Nusselt (Sherwood) number for some values of the buoyancy ratio,  $N$ , and the amplitude,  $A$ .

The velocity profiles for a smooth surface ( $A=0$ ), for  $Pr=0.7$ ,  $Sc=5$  ( $Pr < Sc$ ) and for both negative and positive values of  $N$  at a given  $X$  position ( $X=0.5$ ) are presented in Fig. 2. As shown in this figure, while  $N = -1$ , the two buoyancies oppose each

other and the flow is quiescent. When  $N=4$ , the velocity is positive and the flow is wholly upward. This suggests that for these values of  $N$ , although the boundary layer analysis predicts a reasonably solution. Moreover, for  $N < 0$ , the  $U$ -velocity is negative for  $Y < 0.2$  and positive for  $Y > 0.2$ . Fig. 3 shows that the flow reversal near the surface and this exaggerates the magnitude of the upward velocities; this cannot be accounted as a boundary layer type flow.

For  $Pr=5$ ,  $Sc=0.63$  ( $Pr > Sc$ ), in this case, Fig. 4 shows that the boundary layer analysis gives a reasonable solution for all the values of the buoyancy ratio  $N$ , both positive and negative.

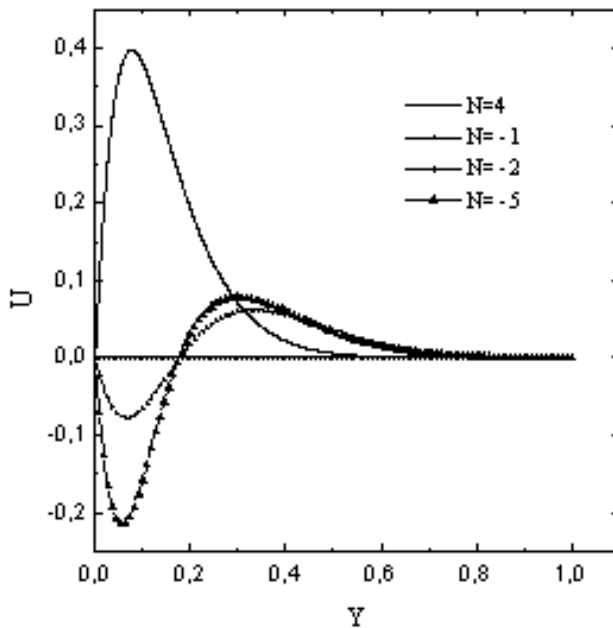


Figure 2: Velocity profile for different buoyancy ratio  $N$  ( $Pr < Sc$ ).

Figure 5 shows the effects of negative buoyancy ratio number  $N$  on the local Nusselt (Sherwood) number and the skin-friction coefficient, respectively, along the wavy surface ( $A=0.3$ ). It is seen from this figure that the decreasing of the negative buoyancy ratio  $N$  leads to a general increase in the heat and mass transfer as well as the local skin-friction coefficient at a given  $X$  position. Furthermore, it is noted from this figure that the maximum values of  $Nu(x)$ ,  $Sh(x)$  and  $Cf(x)$  occur on the crests of the surface while the minimum values occur in the troughs.

Figure 6 illustrates the distribution of the dimensionless temperature and concentration profiles for negative buoyancy ratio  $N$ , where it is seen that the mass boundary

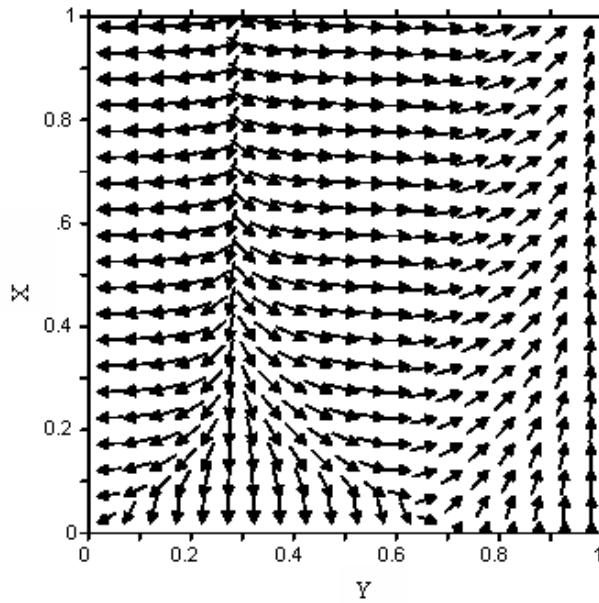


Figure 3: Stream function contours for  $N=-2$ ,  $Pr=0.7$ ,  $Sc=5$  ( $Pr < Sc$ ).

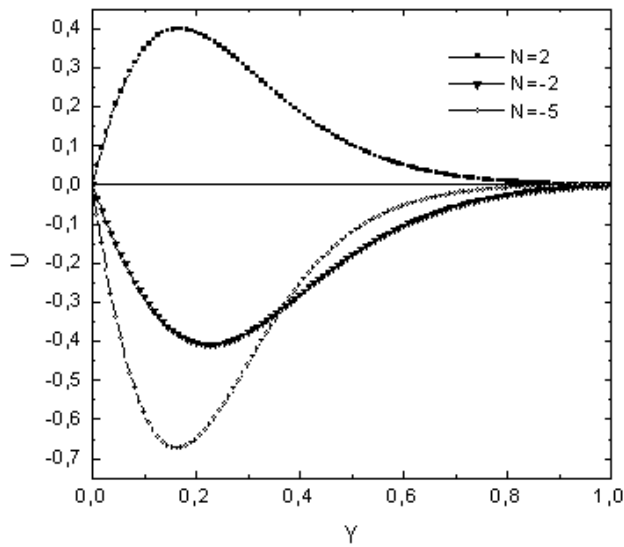


Figure 4: Velocity profile for different buoyancy ratio  $N$ ; ( $Pr=5$ ,  $Sc=0.63$ ).

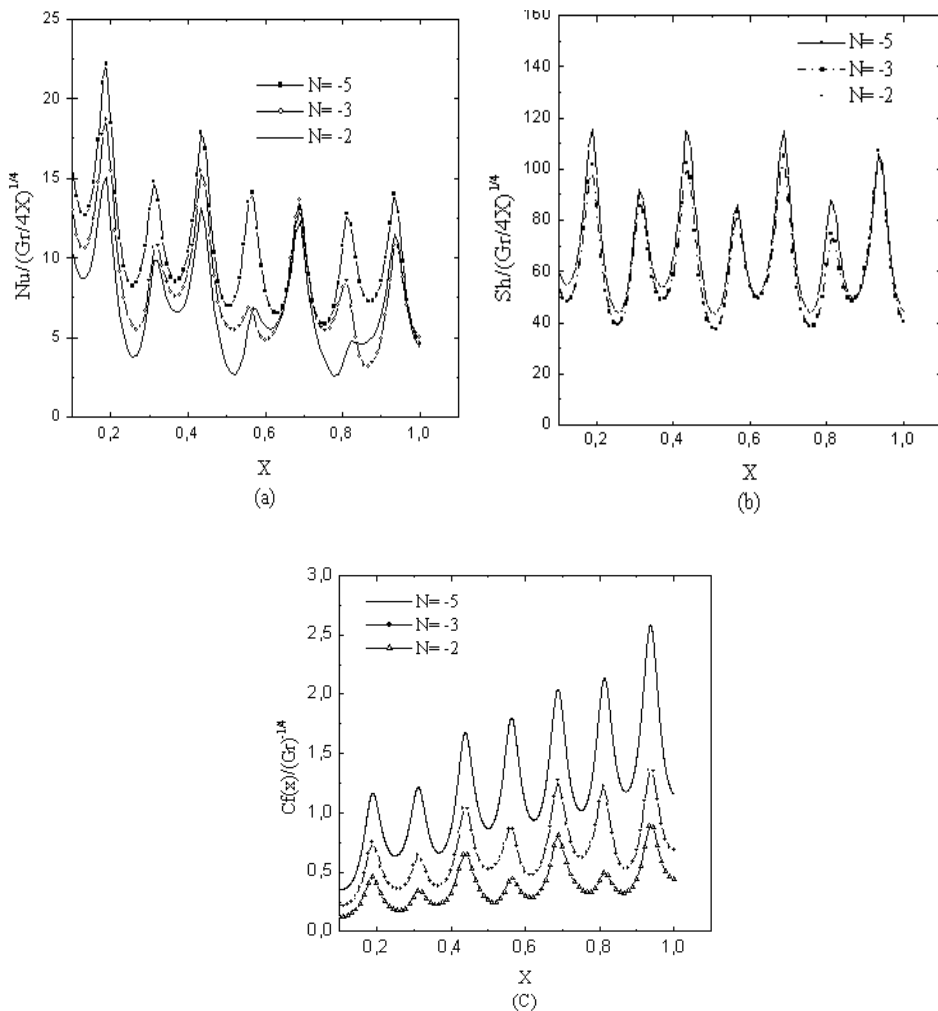


Figure 5: Effects of the buoyancy ratio  $N$  on the axial distributions of Nusselt number; (b) Sherwood number; (c) skin-friction coefficient.

layer thickness is greater than the thermal boundary layer thickness and this is because the thermal diffusion is stronger than the mass diffusion.

The effects of the amplitude wavelength on the heat and mass transfer as well as on the local skin-friction coefficient are reported in Figs. 7 and 8. It is observed that the values of  $Nu(x)$ ,  $Sh(x)$  and  $Cf(x)$  are lower than those of the corresponding flat surface ( $A=0$ ). This may be explained by the observation that an increase in the amplitude decreases both the thermal and the mass buoyancy forces which then

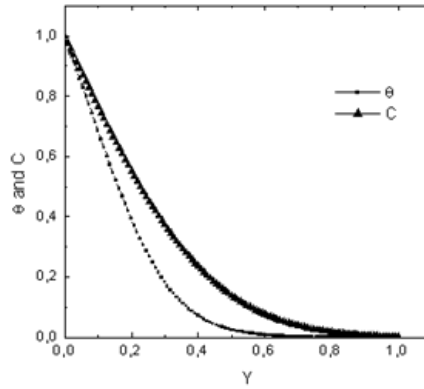


Figure 6: Temperature and concentration profile for  $N = -4$ , ( $Pr > Sc$ ).

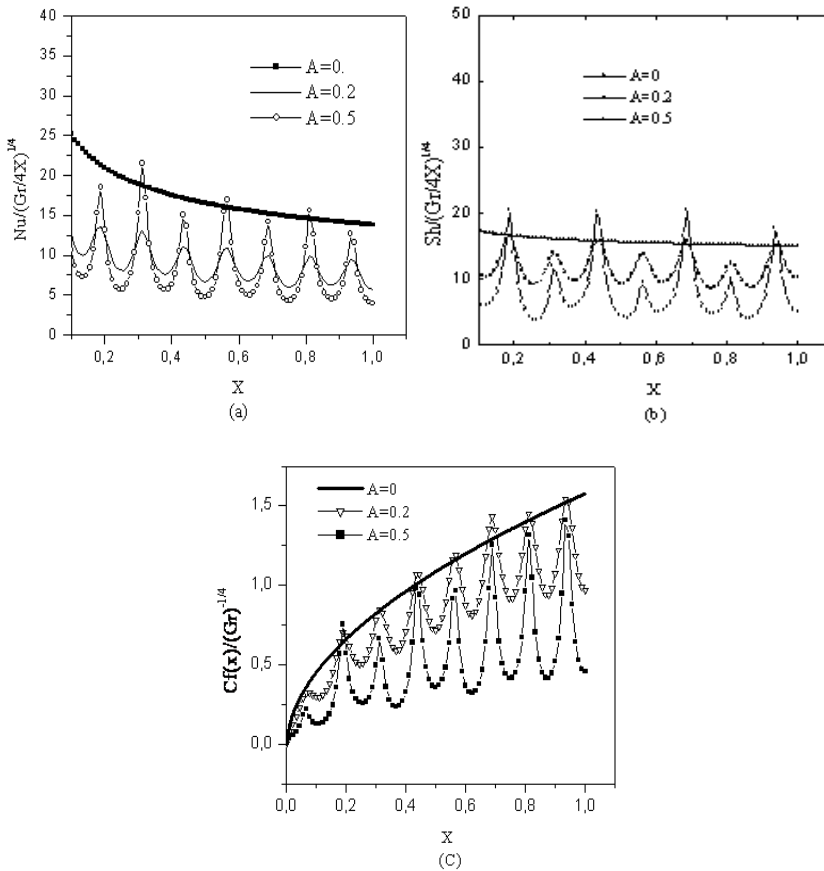


Figure 7: Effects of the amplitude wavelength  $A$  on the axial distributions of : (a) Nusselt number; (b) Sherwood number; (c) skin-friction coefficient.

cause a decrease in the values of  $Nu(x)$ ,  $Sh(x)$  and  $Cf(x)$  in the troughs of the wavy surface.

Figures 8 and 9 depict the effects of the wave amplitude on the development of the isotherms and iso-concentrations. They show a roughly sinusoidal behavior and it is clearly seen that the mass boundary layer thickness is greater than that the thermal boundary layer thickness when  $Pr > Sc$ .

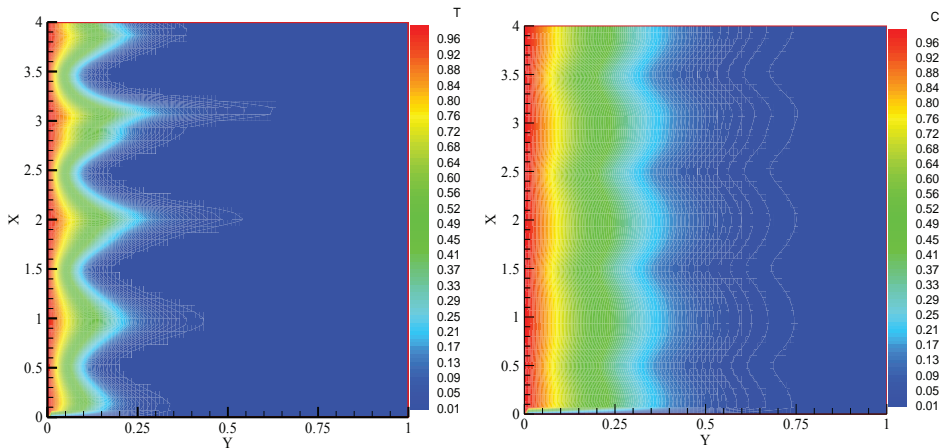


Figure 8: Isotherms for  $A=0.2$  ; ( $Pr > Sc$ ). Figure 9: Iso-concentration for  $A=0.2$  ; ( $Pr > Sc$ ).

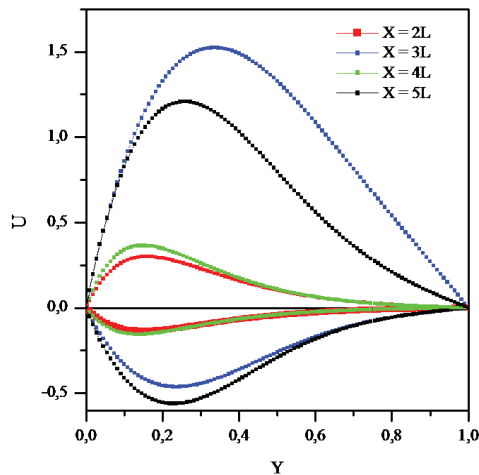


Figure 10: Velocity profile for different wavelength  $L$ .  $N = -3, 3$  and ( $Pr < Sc$ ).

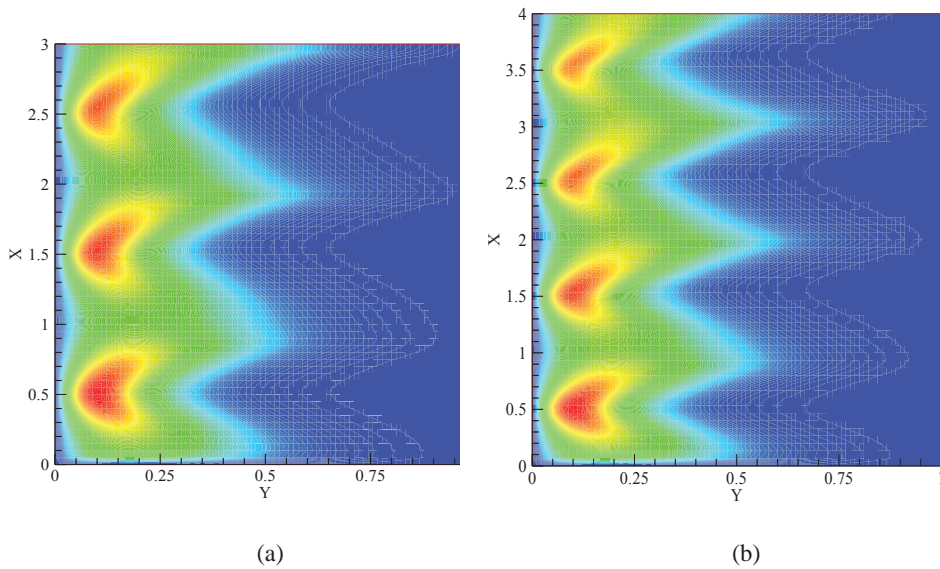


Figure 11: Effects of the wavelength  $L$  on the velocity contours: (a)  $X=3L$  ; (b)  $X=4L$ .

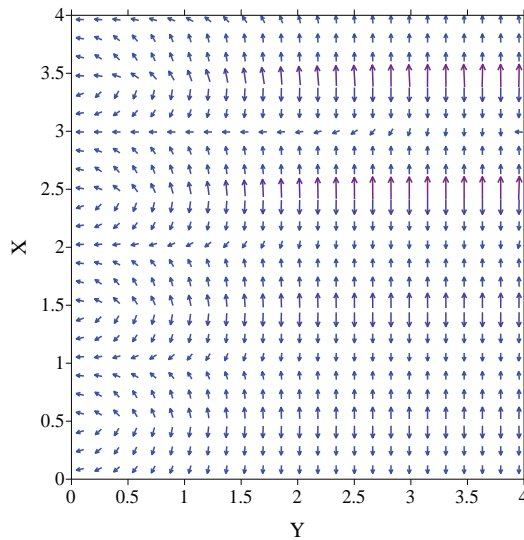


Figure 12: Stream function contours:  $A=0.3$ ;  $N=-3$ .

The effect of the wavelength on velocity profiles is plotted in Fig. 10. In this case, the effect depends to the pair and odd of the wavelength, it is seen that when the wavelength is pair the absolute value of the velocity is week for positive and negative buoyancy ratio, while, when the wavelength is odd the absolute value of the velocity is higher for both the positive or negative buoyancy force. Here, this is because the values of the velocity calculated are in the crests while, when the wavelength is pair, the values of the velocity calculated are in the troughs according to the dimensionless  $X$  ( $X=x/L$ ) as shown in Fig.11.

In addition, for  $Pr < Sc$ ,  $A=0.2$  and  $N=-3$ , it is seen from Fig.12 that the wavy surface perturbs the flow in the crests and in the troughs and we observe recirculation zones in the troughs near the surface.

## 6 Conclusion

Free convection in the boundary layer related to a wavy surface, which is maintained at a constant wall temperature and concentration, has been studied numerically. The physical domain has been transformed using a homotopic function to change the sinusoidal surface into a flat one. The boundary-layer equations have been discretized using a finite volume scheme and solved via Gauss-Seidel iterations.

The results show that boundary layer solutions cannot give exact solutions for  $Pr < Sc$  as already found by some authors. In this case, the flow undergoes reversal near the surface and increases the magnitude of the upward velocities. Concersely, for  $Pr > Sc$ , the boundary layer analysis gives a reasonable solution for all the values of positive or negative buoyancy ratio.

Decreasing the negative buoyancy ratio can be used to increase the heat and mass transfer along the surface. Moreover, an increase in the wavelength leads to a general decrease in the values of the local Nusselt (Sherwood) number and the local skin-friction coefficient.

## References

- Adams, J. A. ; Fadden, Mc.; Aiche, P. W.** (1966): Simultaneous heat and mass transfer in free convection with opposing body forces. *Numer. Heat Transfer, J.* vol. 12, pp. 642-647.
- Al-Ajmi, R. ; Mosaad, M.** (2012): Heat Exchange between film condensation and porous natural convection across a vertical wall. *Fluid Dyn. Mater. Process*, vol. 8, no. 1, pp. 51-68.
- Arid, A.; Kousksou, T.; Jegadheeswaran, S.; Jamil, A.; Zeraouli, Y.;** (2012):

Numerical Simulation of Ice Melting Near the Density Inversion Point under Periodic Thermal Boundary Conditions, *Fluid Dyn. Mater. Process*, vol. 8, no.3, pp. 257-276.

**Bottemanne, F. A.** (1971): Theoretical solution of simultaneous heat and mass transfer by free convection about a vertical flat plate. *Appl. Sci. Res.* vol. 25, pp.137-149.

**Callahan, G. D.; Marner, W. J.** (1976): Transient free convection with mass transfer on a isothermal vertical flat plat. *Int. J. Heat Mass Transfer.*, vol. 19, pp. 165-174.

**Chen, T. S.; Yuh, C. F. ; Motsolgon, A.** (1980): Combined heat and mass transfer in mixed convection along a vertical and inclined plates. *Int. J. Heat and Mass Transfer.* vol. 23, pp. 527-537.

**Chen, T. S.; Yuh, C. F.** (1980): Combined heat and mass transfer in natural convection along a vertical cylinder. *Int. J. Heat and Mass Transfer.* vol.23, pp. 451-461.

**Cheng, C. Y.** (2000): Natural convection heat and mass transfer near a vertical wavy surface with constant wall temperature and concentration in a porous medium. *Int. Comm. Heat and Mass Transfer.* vol. 27, no. 8, pp. 1143-1154.

**Choukairy, K.; Bennacer, R.** (2012): Numerical and Analytical Analysis of the Thermosolutal Convection in an Heterogeneous Porous Cavity. *Fluid Dyn. Mater. Process*, vol. 8, no. 2, pp. 155-172.

**Dihmani, N.; Amraqui, S.; Mezrhab, A.; Laraqi, N.** (2012): Numerical Modelling of Rib Width and Surface Radiation Effect on Natural Convection in a Vertical Vented and Divided Channel. *Fluid Dyn. Mater. Process*, vol. 8, no. 3, pp. 311-322.

**Gebhart, B.; Pera, L.** (1971): The natural of vertical natural convection flows resulting from the combined buoyancy effects of thermal and mass diffusion. *Int. J. Heat and Mass Transfer.* vol. 14, pp. 2025–2050.

**Hamimid, S.; Guellal, M.; Amroune, A.; Zeraibi, N.** (2012): Effect of a Porous Layer on the Flow Structure and Heat Transfer in a Square Cavity. *Fluid Dyn. Mater. Process*, vol. 8, no. 1, pp. 69-90.

**Haslavsky, V.; Miroschnichenko, E.; Kit, E.; Gelfgat, A. Y.** (2013): Comparison and a Possible Source of Disagreement between Experimental and Numerical Results in a Czochralski Model. *Fluid Dyn. Mater. Process*, vol. 9, no. 3, pp. 209-234.

**Hossain, M. A.; Das, S. K.; Rees, D. A. S.** (1998): Heat transfer response of free convection flow from a vertical heated plate to an oscillating surface heat flux. *Act*

*Mechanica*, vol. 126, pp. 101-113.

**Jer-Huan, J.; Wei-Mon, Y.; Hui-Chung, L.** (2003): Natural convection heat and mass transfer along a vertical wavy surface. *Int. J. Heat and Mass Transfer*. vol. 46, pp. 1075–1083.

**Kamath, P. M.; Balaji, C.; Venkateshan, S. P.** (2013): Heat transfer studies in a vertical channel filled with porous medium. *Fluid Dyn. Mater. Process*, vol. 9, no.2, pp. 109-124.

**Shi, K.; Lu, W. Q.** (2006): Time evolution of double-diffusive convection in a vertical cylinder with radial temperature and axial solutal gradients. *Int. J. Heat and Mass Transfer*. vol. 49, pp. 995–1003.

**Mahajan, R. L.; Angirasa, D.** (1993): Combined heat and mass transfer by natural convection with opposing buoyancies. *J. of Heat Transfer*. vol. 115, pp. 606-611.

**Mahmoudi, A.; Mejri, I.; Abbassi, M. A.; Omri, A.** (2013): Numerical Study of Natural Convection in an Inclined Triangular Cavity for Different Thermal Boundary Conditions: Application of the Lattice Boltzmann Method. *Fluid Dyn. Mater. Process*, vol. 9, no.4, pp. 353-388

**Mahrouche, O.; Najam, M.; El Alami, M.; Faraji, M.** (2013): Mixed Convection Investigation in an Opened Partitioned Heated Cavity. *Fluid Dyn. Mater. Process*, vol. 9, no.3, pp. 235-250.

**Mamou, M.** (2003): Stability analysis of the perturbed rest state and of the finite amplitude steady double-diffusive convection in a shallow porous enclosure. *Int. J. Heat and Mass Transfer*. vol. 46, no. 12 , pp. 2263–2277.

**Maougal, A.; Bessaïh, R.** (2013): Heat Transfer and Entropy Analysis for Mixed Convection in Discretely Heated Porous Square Cavity. *Fluid Dyn. Mater. Process*, vol. 9, no.1, pp. 35-58

**Marcoux, M.; Charrier-Mojtabi, M. C.; Azaiez, M.** (1998): Double-diffusive convection in an annular vertical porous layer. *Int. J. of Heat and Mass Transfer*, vol. 42, pp. 2313-2325.

**Markus M.** (2004): Double-diffusive convection: a simple demonstration. *J. Chem. Educ.* vol. 81, no. 4, pp. 526–529.

**Moufekkik, F.; Moussaoui, M. A.; Mezrhab, A.; Naji, H.; Bouzidi, M.** (2012): Numerical Study of Double Diffusive Convection in presence of Radiating Gas in a Square Cavity. *Fluid Dyn. Mater. Process*, vol. 8, no. 2, pp. 129-154.

**Rana, G. C.; Thakur, R. C.** (2013): Effect of Suspended Particles on the Onset of Thermal Convection in Compressible Viscoelastic Fluid in a Darcy-Brinkman Porous Medium. *Fluid Dyn. Mater. Process*, vol. 9, no. 3, pp. 251-266.

**Rtibi, A.; Hasnaoui, M.; Amahmid, A.** (2013): Soret driven thermosolutal convection in an inclined porous layer: search of optimum conditions of separation and validity of the boundary layer theory. *Fluid Dyn. Mater. Process*, vol. 9, no.2, pp. 181-208

**Rudels, B.; Björk, G.; Muench, R. D.; Schaeue, U.** (1999): Double-diffusive layering in the Eurasian basin of the Arctic Ocean. *J. of Marine Research*, vol. 21, pp. 3-27.

**Shemirani, M. M.; Saghir, M. Z.** (2013): An Alternative Approach to Minimize the Convection in Growing a Large Diameter Single Bulk Crystal of Si0:25Ge0:75 Alloy in a Vertical Bridgman Furnace. *Fluid Dyn. Mater. Process*, vol. 9, no.1, pp. 11-22.

**Si-Abdallah, M.; Zeghamati, B.** (2011): Natural Convection Heat and Mass Transfer in the Boundary Layer along a vertical cylinder with opposing buoyancies. *Journal of Applied Fluid Mechanics*, vol. 4, pp. 15-21.

**Yao, L. S.** (1983): Natural convection along a wavy surface. *Asme, J. Heat Transfer*. vol. 105, pp. 465-468.

